

# **Carbon Nanotube Appliques for Fatigue Crack Diagnostics**

Seth S. Kessler, Gregory Thomas, Michael Borgen and  
Christopher T. Dunn

Metis Design Corporation

IWSHM-2015

## **ABSTRACT**

The present research targets hot-spot monitoring for ageing aircraft. The sensor itself is a sheet of CNT sandwiched between two electrically isolating adhesive layers. Any growth of flaw would disrupt the CNT electrical network, therefore increasing the network resistance. This effect would be accentuated if the flaw actually tears through the CNT patch, however since the CNT is piezoresistive, even damage growing under the patch would be measured due to the effective residual strain imparted. Using orthogonal parallel pairs of electrodes, one would be able to not only measure extent of a crack, but also deduce the orientation based on relative changes seen by each pair; a flaw growing towards an electrode would have a small effect, while growing parallel to an electrode pair would offer a significant measured change. Analytical results are presented along with experimental data for calibrated simulated crack growth in addition to actual fatigue crack growth in aluminum specimen.

## **INTRODUCTION**

While more complex Structural Health Monitoring (SHM) methodologies have been demonstrated with various levels of maturity, great benefit could be realized by extremely simple “fuse-style” sensors. In its simplest embodiment, a fuse-style sensor could just be a single conductive trace with a binary response; either a crack has grown long enough to break electrical continuity or not. Multiple traces can be patterned to produce a pseudo-digital response. The present work demonstrates a continuum of crack gauge elements. Specifically, commercially available carbon nanotube (CNT) sheets are employed. CNT-based sensors have great potential for aerospace applications as they are conformal (100 micron applique), lightweight (10 g/m<sup>2</sup>) and can survive extreme environments (over 12000  $\mu\epsilon$  and 500 C). For composite structures they can even be co-cured in a mold as an additional surface ply.

---

Seth S. Kessler, Metis Design Corporation, 205 Portland St, Boston, MA 02114, USA  
Gregory Thomas, Metis Design Corporation, 205 Portland St, Boston, MA 02114, USA  
Michael Borgen, Metis Design Corporation, 205 Portland St, Boston, MA 02114, USA  
Christopher T. Dunn, Metis Design Corporation, 205 Portland St, Boston, MA 02114, USA

CNT have been investigated for a variety of structural, electrical and multifunctional capabilities. In the present study, CNT are embedded into conformal appliques, comprising of surfacing film and electrode layers. The CNT network forms a resistive sheet, and strategically placed electrodes measure the change in resistance across various paths due to damage. Analytical models are used to predict the effect of damage in various locations to optimize the position of electrodes. Damage affects the CNT in two ways. A physical separation in the CNT sheet, such as by a crack, will cause the current between electrode pairs to flow a longer distance, thereby increasing the effective resistance. Sub-surface damage, such as delamination of composite or a yielded/plastic zone in metal, will cause a change in the local strain state, which will stretch or compress the CNT elements and affect the effective network resistance by virtue of their piezoresistivity.

## MODELING

The electrical resistance measured between two electrodes across the CNT sheet was simulated in Matlab. The continuous CNT sheet is divided into an equal spaced, orthogonal array of nodes, which are connected by resistors, as shown in Figure 1. The value of the resistors is a function of the baseline sheet. For an orthogonal and equidistant array of nodes, the value of the resistors connecting each node should be set equal to the local sheet resistivity. This is interesting, as it implies that the analysis is non-dimensional and independent of the actual patch size. The input and output electrodes are connected to the sheet at specified nodes. Both electrodes are given finite resistance values of  $1\Omega$ , and the input is set to 1V while the output is set to 0V. Finally, the mesh of resistors is assembled into a 2D admittance matrix,  $Y$ , and a current source vector,  $I$ , is defined by the input electrode. The voltage at each node on the surface,  $V$ , can then be calculated by multiplying the inverse of  $Y$  by  $I$ . The current supplied by the input electrode is calculated by dividing the difference between the source and input node voltage by the source resistance. The resistance measured between the two electrodes can then be calculated by dividing the difference in the voltage between the input and output nodes, by the input current.

$$\begin{aligned} i_{in} &= (v_s - v_{in}) / R_s \\ R_{measured} &= (v_{in} - v_{out}) / i_{in} \end{aligned} \quad (1)$$

As a crack grows in the metal substrate it also propagates through the CNT sheet bonded to the metal. This results in a local discontinuity in the electrical conductivity of the sheet, which is modelled by a  $1E12$  increase in resistance for the resistors connecting simulation nodes that are separated by the crack. The resistance of the CNT patch is modelled by an  $80 \times 80$  array of nodes. A crack initiates at the center of the plate and grows either parallel, perpendicular or at  $45^\circ$  to the line connected the electrodes. When the crack half-length is 40 nodes, the crack has completely bisected the patch. The change in resistance of the sheet with the growth of the crack for all three cases is shown in Figure 4. It should be noted that the ratio of the  $45^\circ$  change in resistance to the perpendicular change in resistance is not linear with crack length, as would be the case for a rotational projection; this is due to the finite extent of the CNT patch. However, it will be possible using two electrode pairs that are orthogonal to each other to detect the presence and length of a crack no matter what direction.

## **PREDICTION OF SIMULATED FATIGUE CRACK ORIENTATION**

An experiment was devised to predict the extent and orientation of a growing flaw. The specimens were 6x6" 7075 aluminum 1/16" thick plates to be representative of aircraft skin. First a 4x4" piece of surfacing film was placed in the center of each specimen. Next a 3x3" piece of 40 ohm/sq CNT sheet was placed over the surfacing film. Metal mesh was then placed in the center of each of the sides, measuring 1" along the side, 1/4" of overlap on CNT and 1/2" of overlap just on surfacing film. The width was picked using the previously described model as a good balance between sensitivity and coverage across the area based on the shape of the resulting electric field. A piece of surfacing film was placed over the CNT and overlapped mesh, and this entire assembly was vacuum bagged, debulked, and cured at 120°C for 2 hours.

Each specimen was loaded into a custom fixture to support it in a milling machine. A 1/64" carbide end mill was used to simulate crack growth in a specified orientation. First the end mill was plunged into the center of each specimen to create a ~15-mil hole that was 25-mil deep, removed and data was collected. Next the end mill was returned to the hole and moved 20-25 mil at a time using the precision stage to extend the crack, while maintaining a ~15-mil width and 25-mil depth. After each step the bit was retracted and data collected, and this process was repeated 10 times for a maximum flaw of ~1/4" long. Two specimens were machined with cracks parallel to 2 sides, and two specimens were machined with a crack growing along the diagonal.

Figure 5 shows the percentage change for each electrode pair versus crack length. Here the baseline resistance value is subtracted out before normalizing each data point with respect to change in resistance from the baseline condition. Each electrode pair is plotted along with a 2nd order polynomial fit. For the parallel crack growth specimens, there was virtually no change in the perpendicular direction and a very large change in the parallel direction. With the crack growing at a 45°, the electrode pairs had nearly identical percentage changes in resistance, as expected. The datasets overlap at the 2nd point, as the initial hole looks the same to all electrodes.

## **PREDICTION OF ACTUAL FATIGUE CRACK LENGTH**

A second experiment was devised to demonstrate the proposed technology for detecting real crack propagation. Four specimens were prepared in a similar fashion to the previous experiment, however in this case they were in a tensile-coupon format (12" x 1" x 1/8") with just a set of parallel electrodes to conform to a previously developed in-house 4-point fatigue fixture where a stepper motor applies a prescribed displacement at a 1Hz cycling rate supported by outer rollers 8" apart, creating a region of uniform moment between the inner 0.5" spaced rollers. A sharp 1/16" triangular notch was milled from the side of the specimen to introduce a stress concentration for seeding the growth of a fatigue crack. Through a combination of modeling and experimental tuning, it was determined that if loaded at a peak stress of 120% of the yield strength (just at the lower surface since the specimen was in bending), the 6061 aluminum alloy would fail around 18,000 cycles. Three samples were tested as such, with the CNT sensor applied to the tensile surface, and data was collected at the maximum and minimum load point of each cycle. Further, the final sample was cut using the micro-mil to provide a calibration standard of sorts.

Figure 6 shows the CNT resistance change versus notch length along with model predictions, which are in good agreement for cracks over 50-mil. Figure 7 shows the final results for the 3 fatigue crack test specimens, plotting estimated crack length versus cycle number, using model results as the calibration standard. It can be seen that all 3 tests were in close agreement, particularly when the crack was small ( $<0.2''$ ), and that the method appears to have a resolution of roughly  $\pm 0.5$  mil.

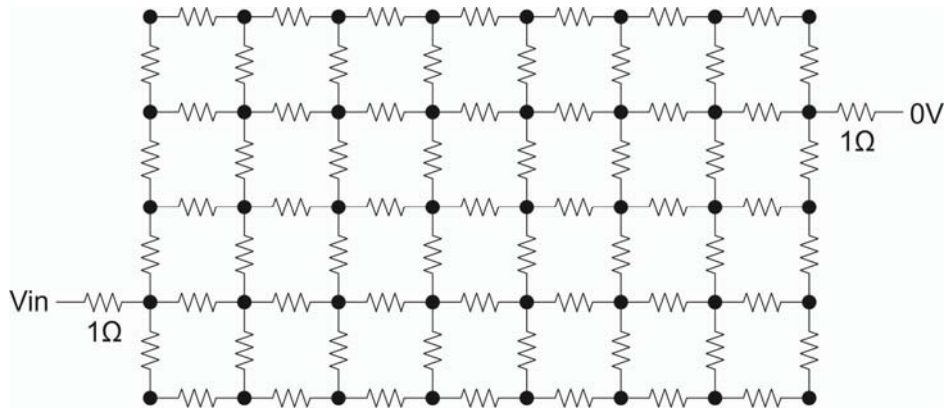


Figure 1. Orthogonal resistor network, with input and output electrodes.

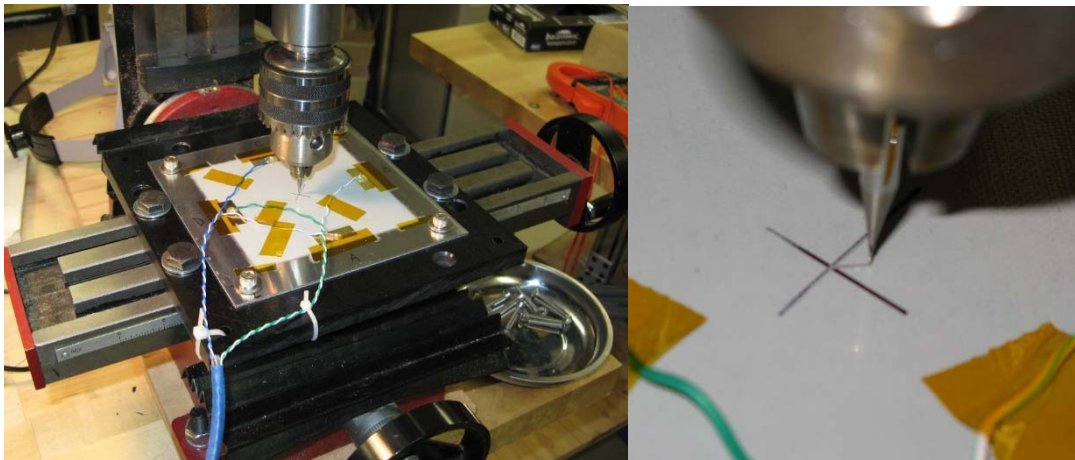


Figure 2. Various photographs of the experimental setup for calibrated flaw detection

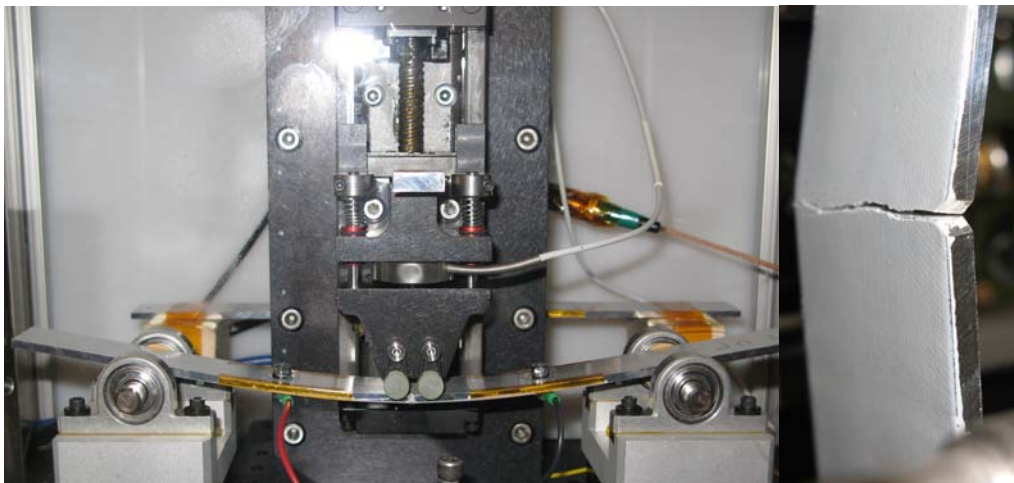


Figure 3: Various photograph of 4-pt fatigue bend fixture and fatigue crack growth

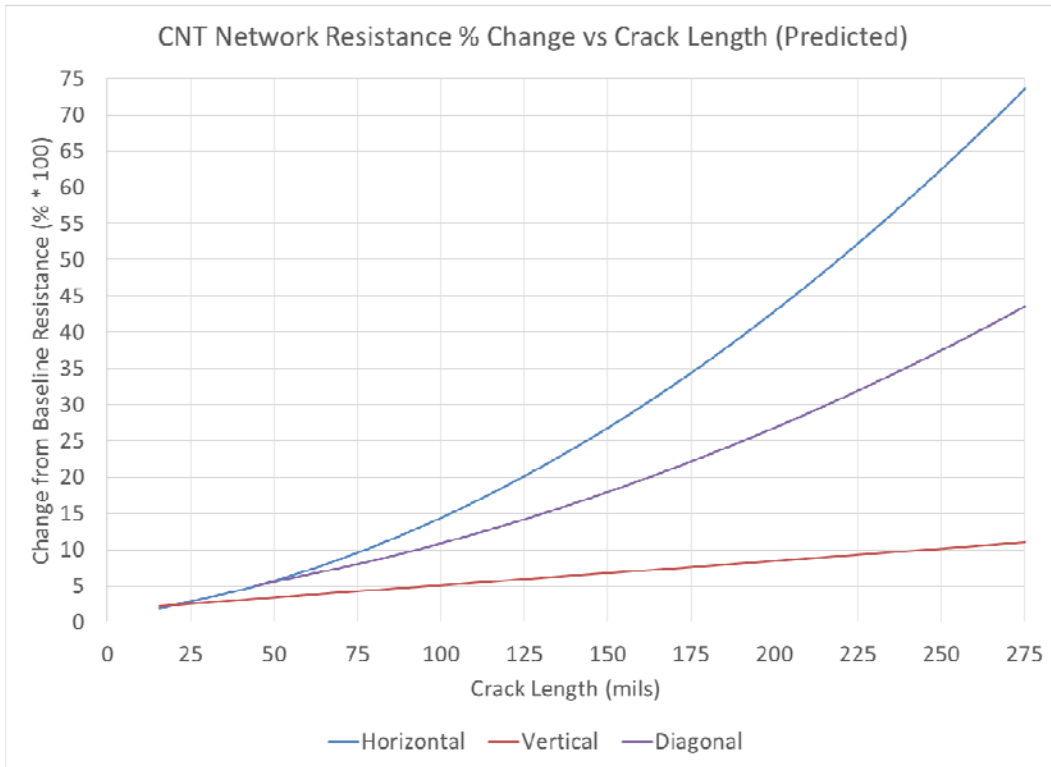


Figure 4. Predicted change in CNT patch resistance with crack length.

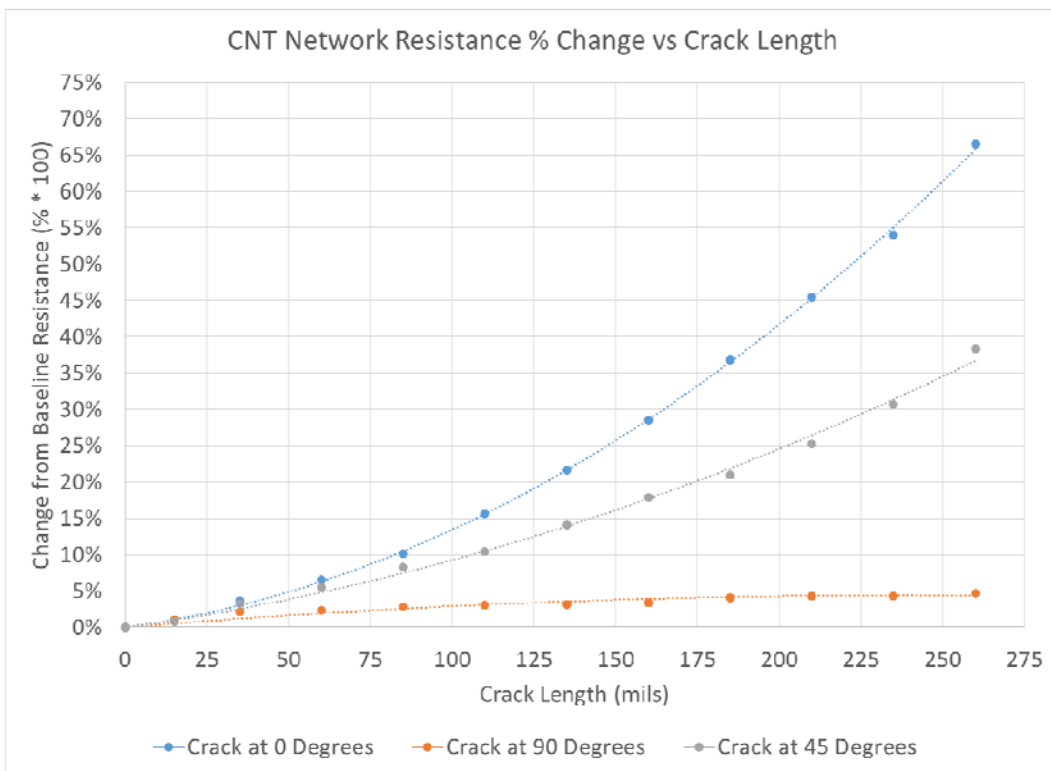


Figure 5: Percentage change plot for milled specimens, fit with 2<sup>nd</sup> order polynomials

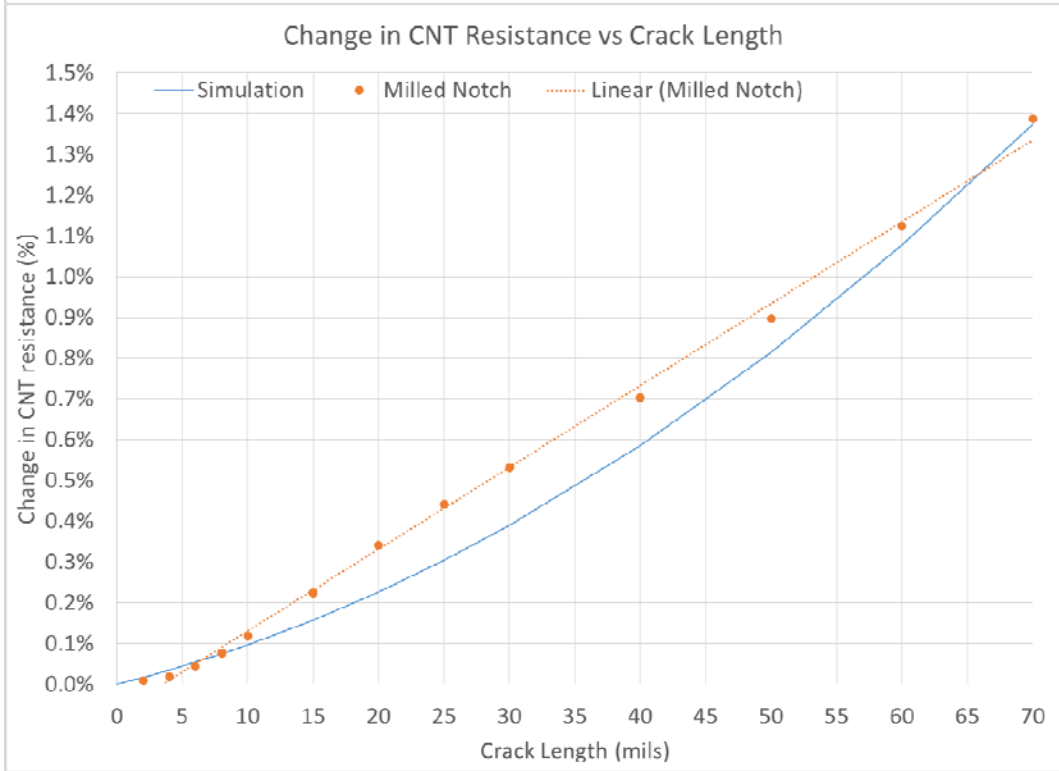
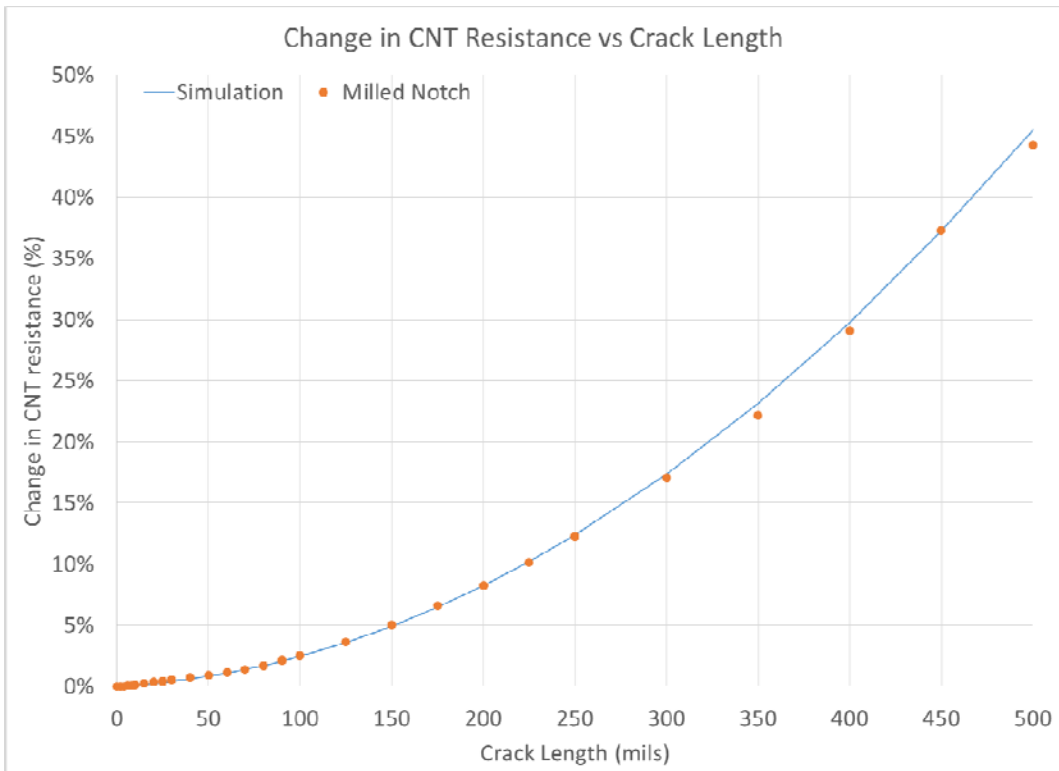


Figure 6: CNT resistance change versus milled notch depth along with simulation results, all data (top) & zoomed view (bottom). Model closely matches response due to calibrated machined notch within the resolution of model elements (1/16")

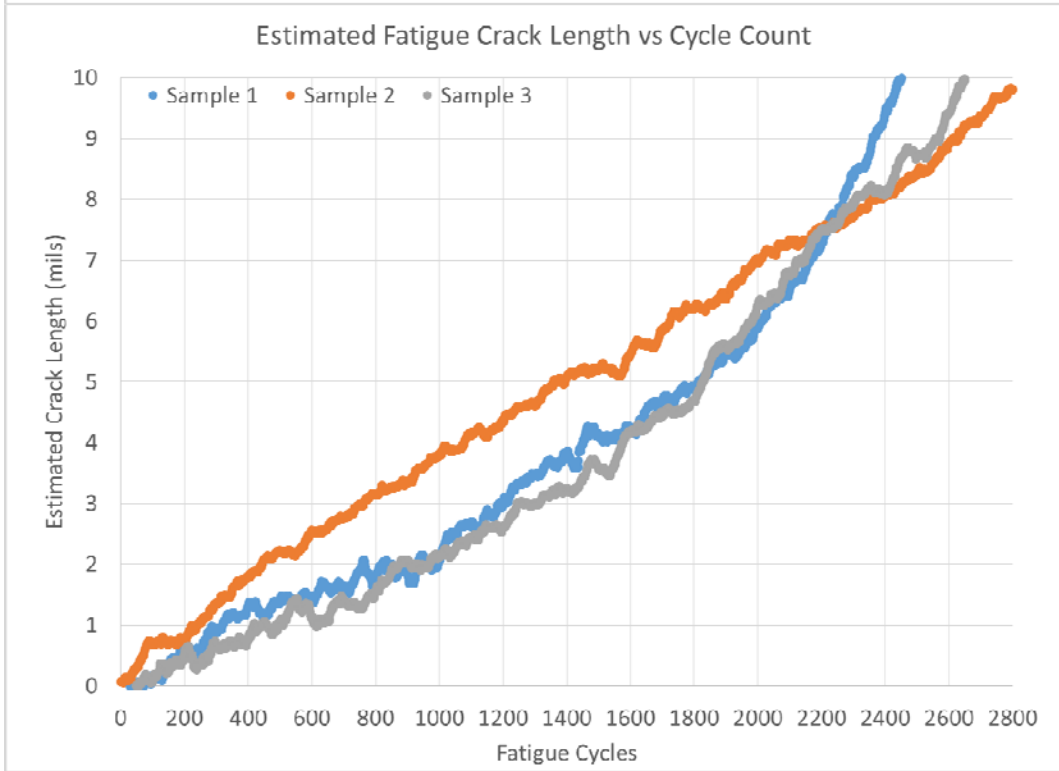
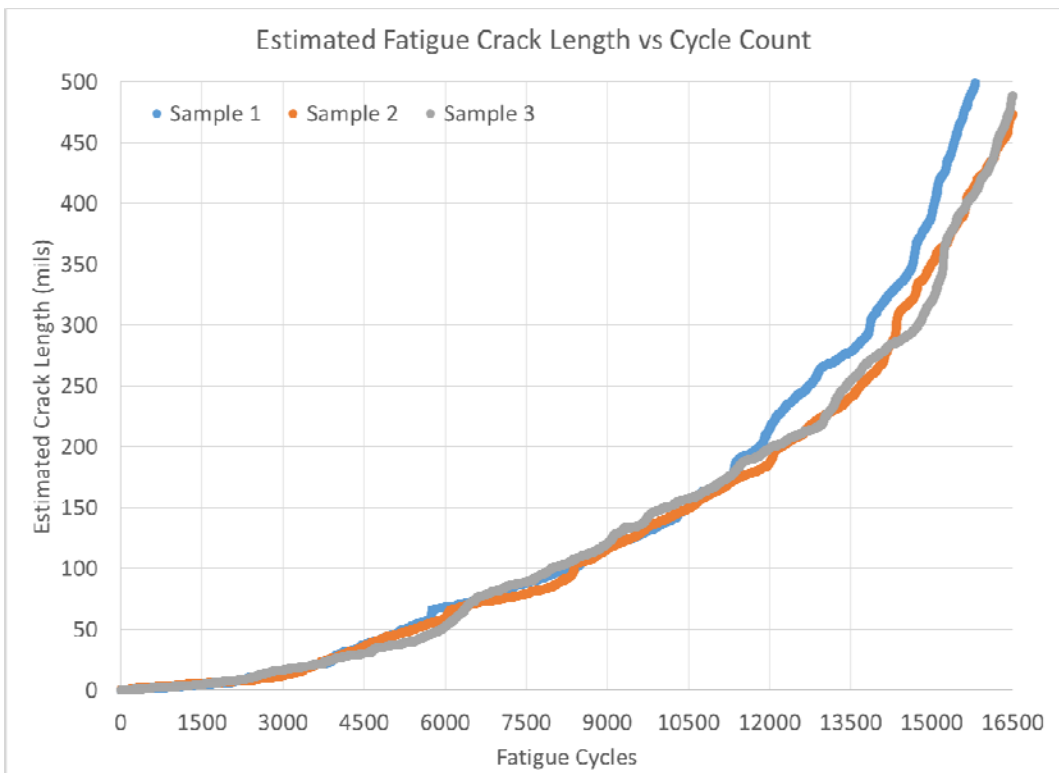


Figure 7: Estimated crack length versus cycles for all fatigue specimens, all data (top) & zoomed view (bottom). Crack estimates were predicted based on model calibration from Figure 6 and are in close agreement with each other.



## CONCLUDING REMARKS

The initial set of tests were able to demonstrate a clear and reproducible response to the growing 15-mil milled notch, both in terms of size and orientation using the orthogonal electrode pairs. Raw data was presented as a percentage change in resistance, without need for any signal processing or algorithms to interpret the results, which closely matched the model predictions. A model was constructed to produce predictions for the crack length versus CNT resistance change. A specimen was cut using a 15-mil end-mill to validate the model, which was in excellent agreement. Thus the results for fatigue crack specimens was plotted using this calibration, where all specimen were in close agreement for fatigue behavior, particularly up through 0.2". Even in the zoomed in view (up to 0.01") they are within 0.002" at any given cycle, which is not terribly surprising for high-tolerance aluminum specimen with a major stress concentration. Therefore it can be deduced that the presented method is reliably sensitive to cracks as small as 0.001" with a tolerance of  $\pm 0.0005$ ", at least for the given setup. Overall, this approach shows many benefits over competing technologies such as simplicity of usage and the straightforward results.

## ACKNOWLEDGMENTS

This research was performed at the Metis Design Corporation in Boston, MA, and sponsored by the Office of Naval Research, under the SBIR contract N00014-12-C-0316 and the Air Force Research Laboratory under SBIR contract FA8650-14-M-2480.

## REFERENCES

1. Garcia E.J., Wardle B.L., Hart J.A. and Yamamoto N., "Fabrication and multifunctional properties of a hybrid laminate with aligned carbon nanotube" *Composite Science and Technology*, v. 68, pp. 2034-41, 2008.
2. Raghavan A., Kessler S.S., Dunn C.T., Barber D., Wicks S. and B.L. Wardle. "Structural Health Monitoring using Carbon Nanotube (CNT) Enhanced Composites." *Proceedings of the 7th International Workshop on Structural Health Monitoring*, 9-11 September 2009, Stanford University.
3. Wicks S., Barber D., Raghavan A., Dunn C.T., Daniel L., Kessler S.S. and B.L. Wardle. "Health Monitoring of Carbon NanoTube (CNT) Hybrid Advanced Composite for Space Applications." *Proceedings of the 11th European Conference on Spacecraft Structures*, September 2009 Toulouse, France.
4. Barber D., Wicks S., Wardle B.L., Raghavan A., Dunn C.T. and S.S. Kessler. "Health Monitoring of CNT Enhanced Composites." *Proceedings of the SAMPE Fall Technical Conference*, October 2009, Wichita, KS.
5. Kessler S.S., Raghavan A., Dunn C.T., Wicks S., Guzman deVilloria R., and B.L. Wardle "Fabrication of a Multi-Physics Integral Structural Diagnostic System Utilizing Nano-Engineered Materials." *Proceedings of the 2nd Annual Conference of the Prognostics and Health Management Society*, October 2010, Portland, OR.
6. Wicks, S., Raghavan, A., Guzmán de Villoria, R., Kessler, S.S., and B.L. Wardle, "Tomographic Electrical Resistance-based Damage Sensing in Nano-Engineered Composite Structures," *AIAA-2010-2871, 51<sup>st</sup> AIAA Structures, Structural Dynamics, and Materials (SDM) Conference*, Orlando, FL, April 12-15, 2010.
7. Guzman de Villoria, R., Kessler, S.S., Yamamoto, N., Miravete, A., and B.L. Wardle. "Multi-Physics Nano-engineered Structural Damage Detection and De-icing." *Proceedings of the 18th International Conference on Composite Materials*, 21-26 August 2011, South Korea.
8. Kessler S.S., Dunn C.T., Wicks S., Guzman deVilloria R. and B.L. Wardle. "Carbon Nanotube (CNT) Enhancements for Aerosurface State Awareness." *Proceedings of the 8th International Workshop on Structural Health Monitoring*, 12-15 September 2011, Stanford University.
9. Guzmán de Villoria, R., Yamamoto, N., Miravete, A., and B.L. Wardle, "Multi-Physics Damage Sensing in Nano-Engineered Structural Materials," online in *Nanotechnology*, April 2011.
10. Kessler S.S., Thomas G., Borgen M. and C.T. Dunn. "Performance Analysis for CNT-based SHM in Composite Structures." *Proceedings of the 9th Int'l Workshop on SHM*, September 2013, Stanford University.